Report of LCLS-II Injector Solenoid Measurements

Feng Zhou

for Scott Anderson & Mark Woodley

October 11, 2017

## 1. INTRODUCTION

Two solenoids magnets (barcodes 4050 & 4051) for LCLS-II injector have been measured at SLAC by Scott Anderson. The measurements followed the solenoid measurement plan (developed by Dave Dowell) shown in Figure 1. In this document, we summarized the field measurements (via hall probe, long rotating coil, and short rotating coil) for the two solenoids. Note solenoid barcodes 4051 and 4050 are assigned to the first solenoid (SOL1) and the second solenoid (SOL2) in the beamline, respectively.

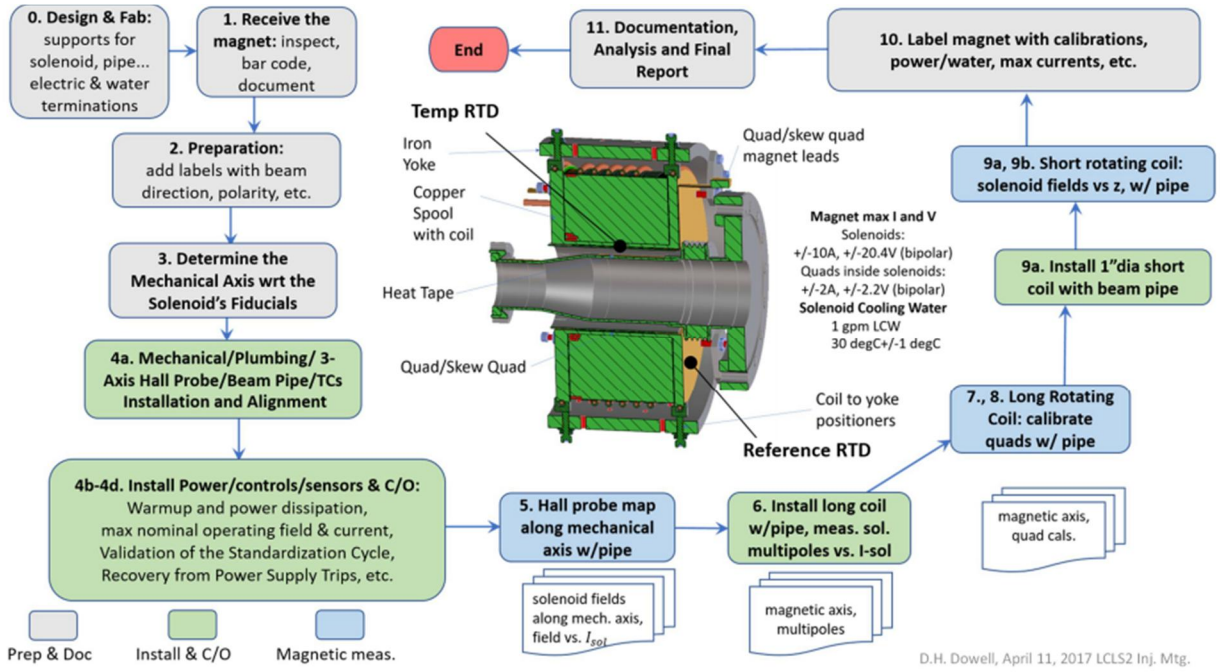


Figure 1: Solenoid field measurement plan.

## 2. MAGNETIC FIELD MEASUREMENTS

### 2.1 Hall Probe Measurements

Hall probe measurements for the two solenoids with their original vacuum chambers are shown in Figures 2 and 3 respectively. Figures 2 & 3 (left) show the $B_z$ vs. z for different solenoid current I with 1-axis hall probe. Figures 2 & 3 (right) show the measured $B_z * L_{eff}$ (at z=0 position) vs. I, where $L_{eff}$ is extracted from the data shown in Figures 2 & 3 (left). The fitted linear polynomial coefficients, "p1", will be used in the control system to convert desired length-integrated field, $B_z*L_{eff}$, to excitation current, I.

Figures 4 & 5 show the measured $B_x$ and $B_y$ vs. z with 3-axis hall probe, for both solenoids at different currents. We do not have tolerances for the Bx and By so these measurements shown in Figures 4 & 5 are used for reference only.

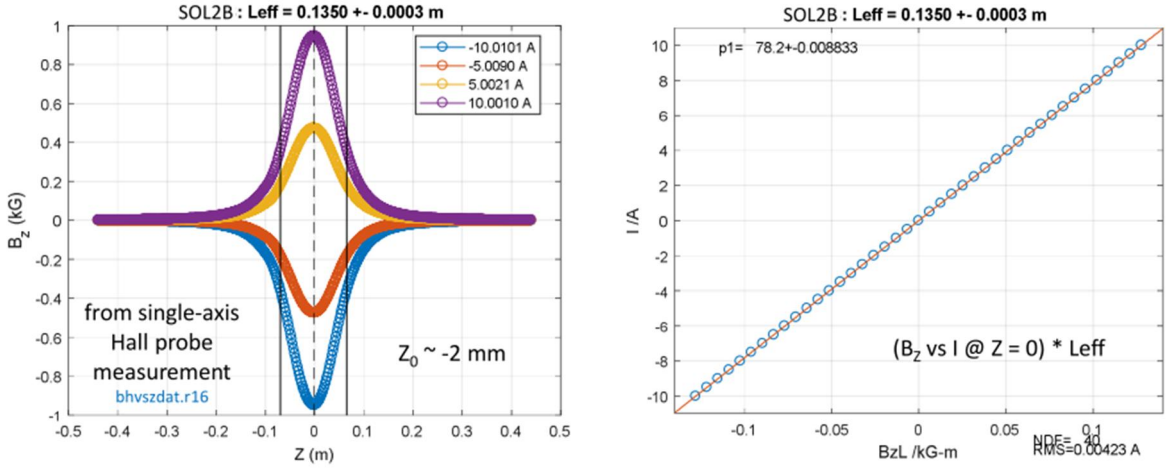


Figure 2: Measured $B_z$ vs. z for different solenoid current (left) and $B_z$*$L_{eff}$ vs. current I (right) for solenoid barcode 4050 (SOL2). The polynomial coefficient, "p1", is in units of A/kG-m.

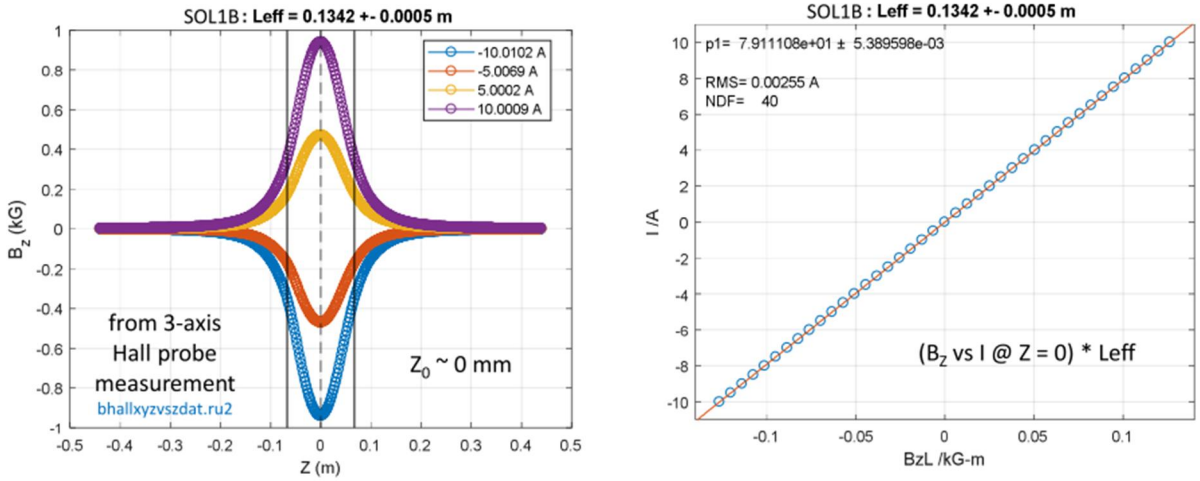


Figure 3: Measured $B_z$ vs. z for different solenoid current (left) and $B_z$*$L_{eff}$ vs. current I (right) for solenoid barcode 4051 (SOL1). The polynomial coefficient, "p1", is in units of A/kG-m.

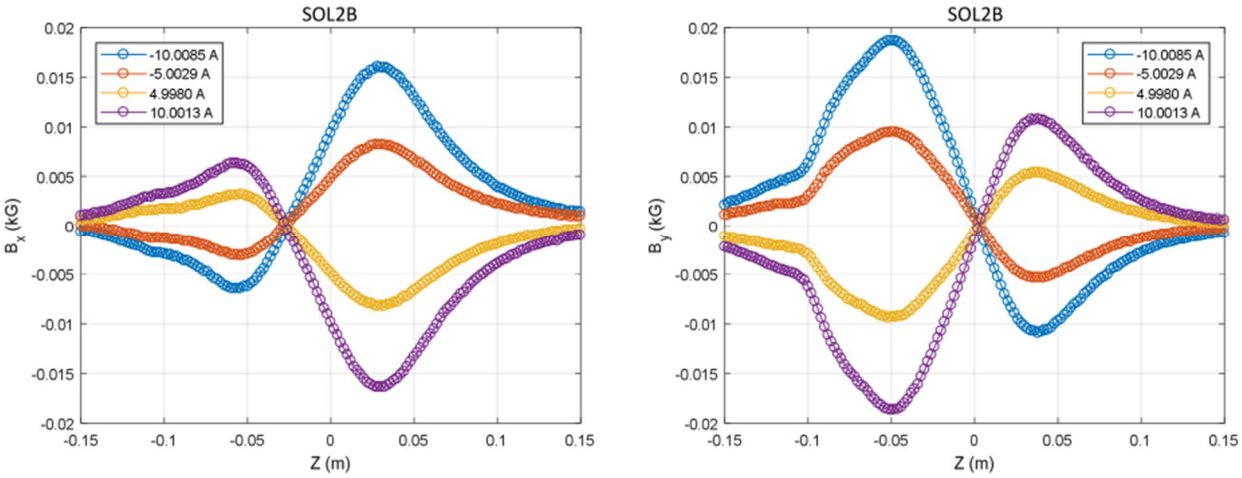


Figure 4: $B_x$ (left) and $B_y$ (right) vs. z at different currents for solenoid barcode 4050 (SOL2). These measurements are used for reference only.

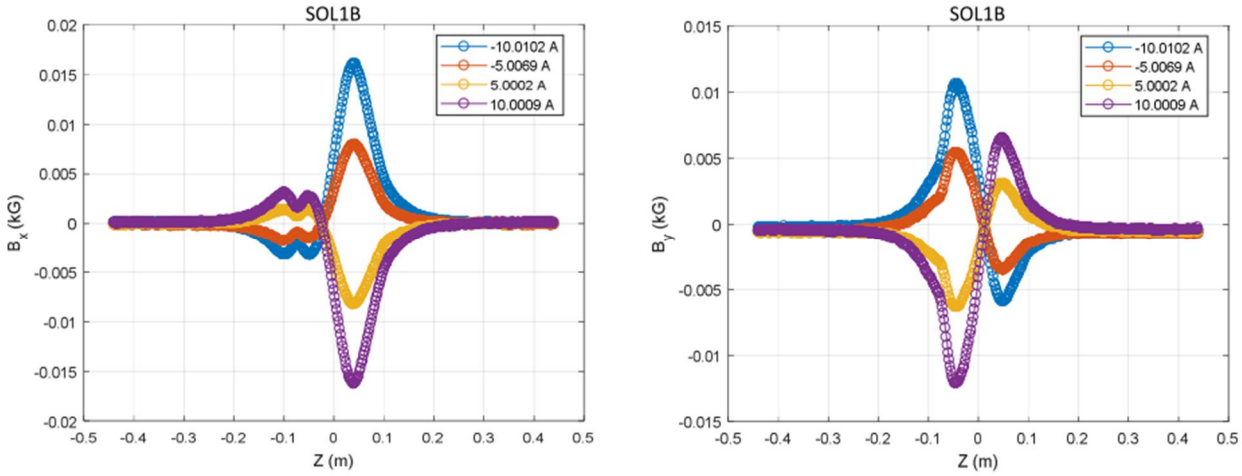


Figure 5: $B_x$ (left) and $B_y$ (right) vs. z at different currents for solenoid barcode 4051 (SOL1). These measurements are used for reference only.

## 2.2 Long Rotating Coil Measurements

Harmonic fields, including quadrupole and sextupole, were measured with a long rotating coil, as shown in Figures 6 & 7, for each solenoid operating at 10 A (nominal current is ~6 A), respectively. One normal quadrupole (CQ) and one skew quadrupole (SQ) are imprinted on the center of each solenoid chamber to compensate the quadrupole effect caused by solenoid/chamber itself. The CQ and SQ integrated fields were each calibrated with a long rotating coil, as shown in Figures 8 & 9 for the two solenoids, respectively. Figures 10 & 11 show the quad compensation. All above fields are measured for the solenoid with the original vacuum chamber in place.

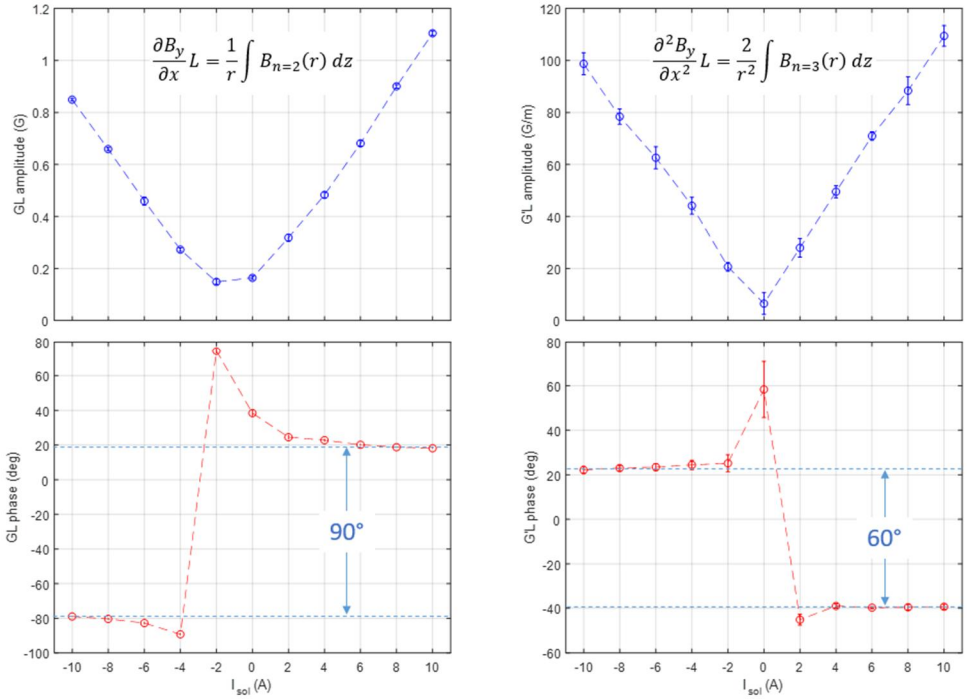


Figure 6: Measured quadrupole (left) and sextupole (right) for the solenoid 4050 (SOL2) at 10 A (nominal operation current is 6 A) with the original chamber.

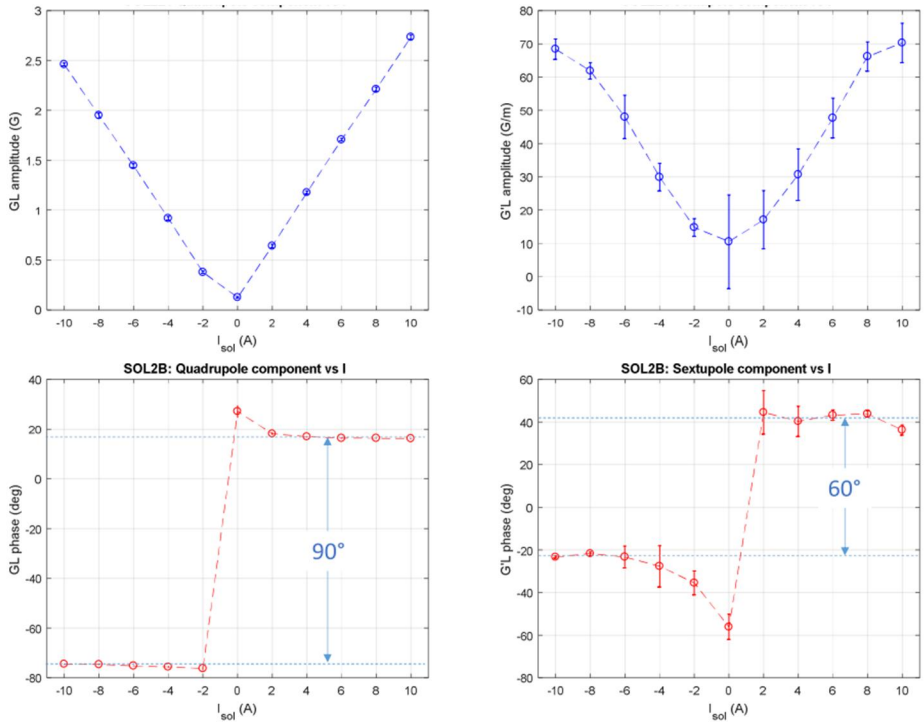


Figure 7: Measured quadrupole (left) and sextupole (right) for the solenoid 4051 (SOL1) at 10 A (nominal operation current is 6 A) with the original chamber.

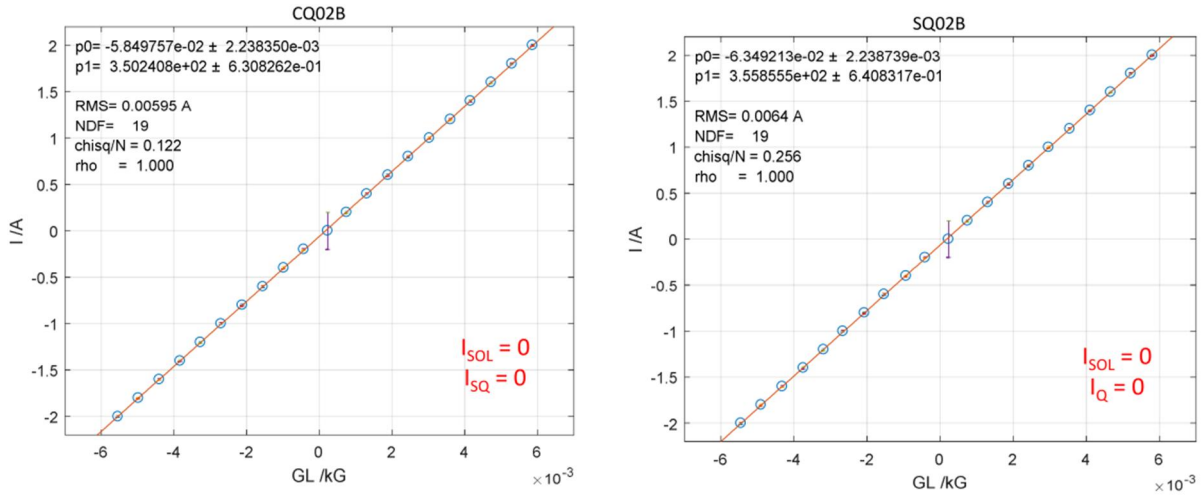


Figure 8: Measured CQ (left) & SQ (right) integral field vs. quadrupole current for solenoid 4050 (SOL2). The fitted polynomials, "p0" & "p1" are used to convert desired field to excitation current.

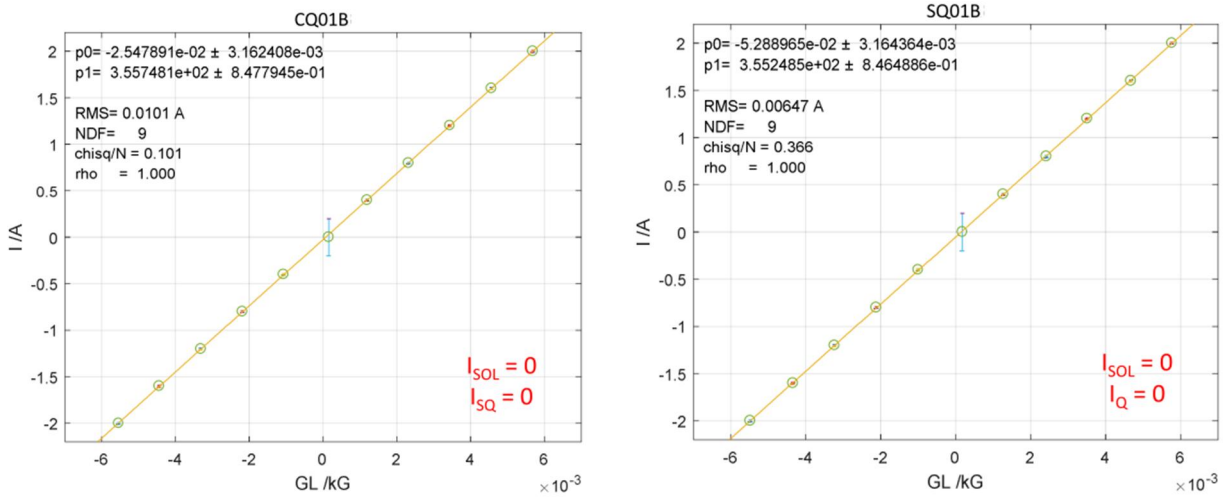


Figure 9: Measured CQ (left) & SQ (right) integral field vs. quadrupole current for solenoid 4051 (SOL1). The fitted polynomials, "p0" & "p1" are used to convert desired field to excitation current.

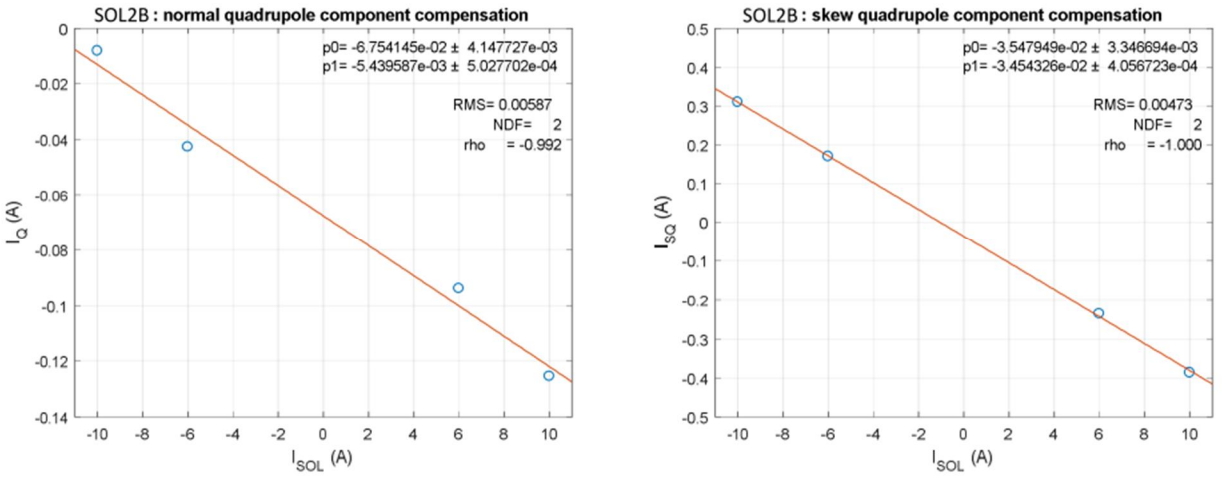


Figure 10: CQ (left) and SQ (right) current vs. solenoid current for compensation of quadrupole field caused from solenoid 4050 (SOL2). This solenoid's nominal current is ~4A.

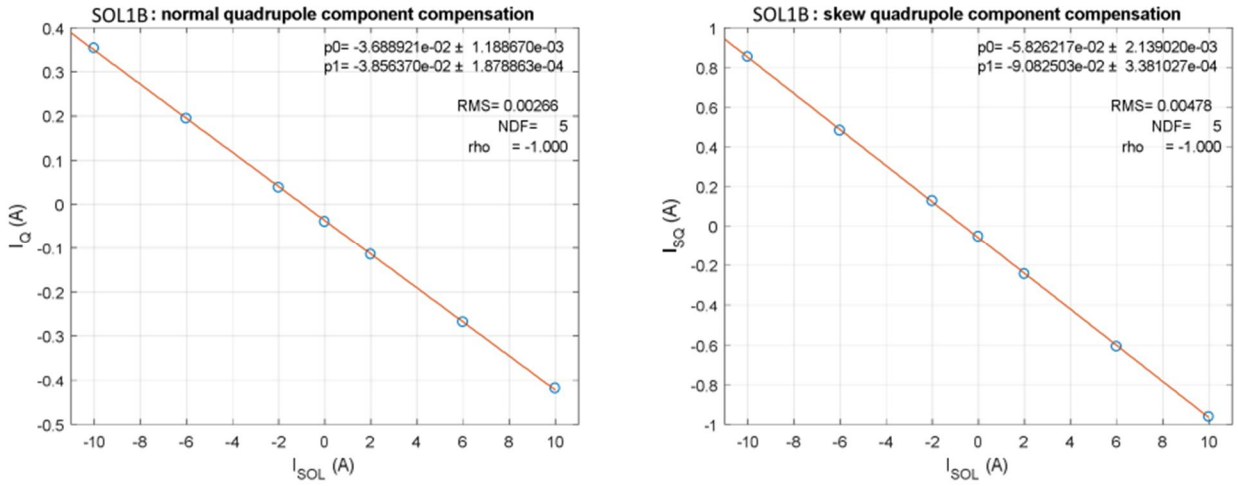


Figure 11: CQ (left) and SQ (right) current vs. solenoid current for compensation of quadrupole field caused from solenoid 4051 (SOL1). This solenoid's nominal current is ~6 A.

## 2.3 Short Rotating Coil Measurements

The sextupole field from the solenoid with the original vacuum chamber was measured with the short-coil. Simulations with the measured short-coil sextupole field show significant emittance growth. It was later found that the solenoid vacuum chamber was magnetic on the welded flange areas for both solenoids. After annealing the chambers at 1050°C for 15 min, the stray magnetic effect disappeared as measured with a hall probe. We measured the sextupole field again, for the solenoids with annealed chambers, with the short-coil. The sextupole field for the solenoid with the annealed chamber was significantly reduced, in comparison to the original chamber, as shown in Figure 12. The emittance

growth is negligible with the sextupole field for the solenoid with the annealed chamber. Similar results were observed for the other solenoid. Sextupole field measurements using a long coil for the solenoid without a vacuum chamber is about 10% lower than the one with the original vacuum chamber.

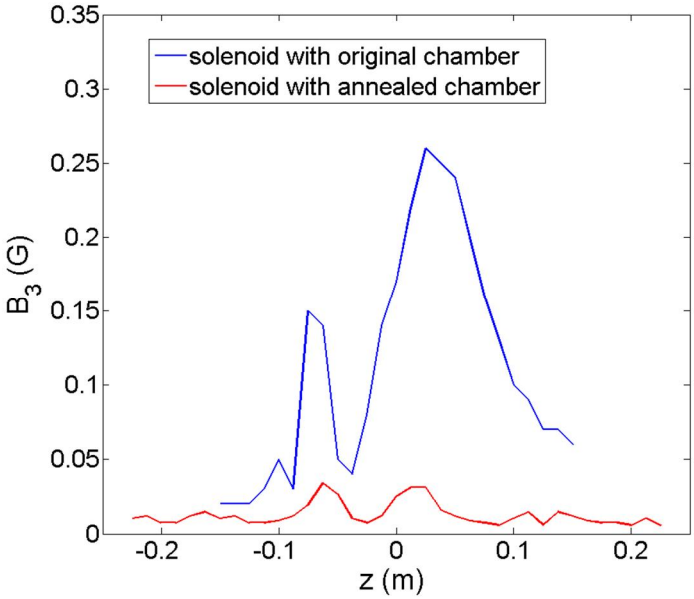


Figure 12: Measured sextupole field (via short-coil) for the solenoid 4051 (SOL1) with the vacuum chamber.

## 3. SUMMARY

The magnetic field measurements for the two solenoids and corresponding quadrupoles are summarized in the following tables.

Table 1: Solenoid 4050 (SOL2) field measurements.

| Parameters | specification | measured |
|---|---|---|
| Max. longitudinal physical size | 17.4 cm | |
| Effective length $(\frac{1}{B_0}\int B_z\,dz)$ | 12.9 | 13.5 cm |
| Max current | 10 A | 10 A |
| Maximum field, $B_0$ @10A | 1075 G | 947 G |
| Min. beam pipe inner radius | 23.75 mm | 23.75 mm |
| Min. bore radius | 33 mm | |
| Max. Focal Strength $(\int B_z^2\,dz)$ | $10^{-3}$ $T^2$ m | $7.8\text{x}10^{-4}$ $T^2$ m |
| Min. focal distance at 750 keV | 5.5 cm | 2.1 cm |
| Remote alignment control of Δx, Δy | +/- 3 mm | |
| Remote alignment control of x' and y' | +/- 30 mrad | |
| Power supply relative stability (r.m.s.) | $<10^{-4}$ | |
| Good field region radius | 10 mm | 10 mm |
| Max integrated quadrupole field $(\frac{\partial B_y}{\partial x} L_{eff,quadrupole})$ | 5 G | 0.8 G |
| Max integrated sextupole field $(\frac{\partial^2 B_y}{\partial x^2} L_{eff,sextupole})$ | 55 G/m | 52 G/m |

Table 2:Measured quadrupole and skew quadrupole in the solenoid 4050 (SOL2).

| | specification | measured |
|---|---|---|
| Max field @2A (@6mm radius) | 0.59 G | 0.64 G |
| Magnet length | 55 mm | |
| Max integrated field | 5.4 G @2A | 5.8 G @2A |
| gradient @2A | 1 G/cm | 1.07 G/cm |
| Good field region radius | 10 mm | 10 mm |
| Max current | 2 A | 2 A |
| P.S relative stability | < 0.1% | |

Table 3: Solenoid 4051 (SOL1) field measurements.

| Parameters | specification | measured |
|---|---|---|
| Max. longitudinal physical size | 17.4 cm | |
| Effective length (definition sees Table 1) | 12.9 cm | 13.42 cm |
| Max current | 10 A | 10 A |
| Maximum field, $B_0$ @10A | 1075 G | 942 G |
| Min. beam pipe inner radius | 23.75 mm | 18.16-23.75 mm |
| Min. bore radius | 33 mm | |
| Max. Focal Strength (definition sees Table 1) | $10^{-3}$ T$^2$m | 7.6x$10^{-4}$ T$^2$m |
| Min. focal distance at 750 keV | 5.5 cm | 2.1 cm |
| Remote alignment control of Δx, Δy | +/- 3 mm | |
| Remote alignment control of x' and y' | +/- 30 mrad | |
| Power supply relative stability (r.m.s.) | $<10^{-4}$ | |
| Good field region radius | 10 mm | 10 mm |
| Max integrated quadrupole field ($\frac{\partial B_y}{\partial x} L_{eff,quadrupole}$) | 5 G | 1.6 G |
| Max integrated sextupole field ($\frac{\partial^2 B_y}{\partial x^2} L_{eff,sextupole}$) | 55 G/m | 44.4 G/m |

Table 4: Measured quadrupole and skew quadrupole in the solenoid 4051 (SOL1).

| | specification | measured |
|---|---|---|
| Max field @2A (@6mm radius) | 0.59 G | 0.60 G |
| Magnet length | 55 mm | |
| Max integrated field | 5.4 G @2A | 5.5 G @2A |
| gradient @2A | 1 G/cm | 1.0 G/cm |
| Good field region radius | 10 mm | 10 mm |
| Max current | 2 A | 2 A |
| P.S relative stability | < 0.1% | |